Collectivity and thermalization in p+p, p+A, d+Au and ^{3}He+Au collisions

Shengli Huang

Department of Physics and Astronomy, Station B 1807, Vanderbilt University, Nashville, TN 37235, USA

E-mail: shengli.huang@vanderbilt.edu

Abstract. In this proceeding, the recent measurements of the anisotropy(v_2, v_3) in small collision systems such as p+p, p+A, d+Au and ^{3}He+Au collisions at the LHC and RHIC energies are presented. In p+p collisions, the v_2 are measured by two and multi-particle $\Delta\phi$ correlations at $\sqrt{s_{NN}}$ = 2.76, 5, 7, and 13 TeV. In 200 GeV p+Au, d+Au and ^{3}He+Au collisions. the v_2 are measured with event plane methods. I also present the measurements of v_2 for K^0_S and $\Lambda/\overline{\Lambda}$ in high multiplicity p+p collisions, in which a particle mass ordering is observed. The v_2 of identified $\pi^{\pm}$, $K^{\pm}$ and(anti)protons in central ^{3}He+Au collisions are also measured and quark-number scaling is observed. These observations are similar to those seen in A+A collisions, and support the interpretation of a collective origin.

1. Introduction

Recently, in the high-multiplicity small collision systems such as p+p and $p/d/^3$He+A collisions, the near-side, long-range two particle angular correlation (so called 'ridge') and anisotropic flow (v_n) have been observed at the LHC [1, 2, 5, 3, 4] and RHIC [6, 7, 8]. Several physics models, which include initial-state gluon saturation [9], and hydrodynamic flow from a mini-QGP(Quark Gluon Plasma) [10] are potential explanations for these observations. While the former will not depend on the initial geometry, the hydrodynamic models have strong initial geometry dependence. Therefore, measuring the v_2 and v_3 in $p/d/^3$He+Au collisions will provide direct testing for these explanations since the initial geometry is quite different for these collisions [11]. If a mini-QGP exists in the small collision system, studying it will help us to further understand: 1)the condition for the QGP thermalization; 2)the role of the internal structure of proton on the initial geometry eccentricity [12]; and 3)the contributions from pre-equilibrium stage to the system evolution [13].

2. The v_2 measurements in p+Au, d+Au and ^{3}He+Au collisions at $\sqrt{s_{NN}}$ = 200 GeV at RHIC

The v_2 for inclusive charged hadrons produced at mid-rapidity $|\eta| < 0.35$ are measured in 0-5% central p+Au in the PHENIX experiment and compared with that from d+Au and ^{3}He+Au collisions, as shown in the Fig. 1. The v_2 in the p+Au is found to be smaller than that of d+Au and ^{3}He+Au. The eccentricity of p+Au is also smaller than that of d+Au and ^{3}He+Au. It indicates the anisotropy in the small collisions system depends on the initial geometry, which is supported by the hydrodynamic model calculation [13] as shown in the figure.

The v_3 for inclusive charged hadrons produced at mid-rapidity $|\eta| < 0.35$ in high-multiplicity ^{3}He+Au collisions at $\sqrt{s_{NN}} = 200$ GeV are also measured in the PHENIX experiment with respect to the Ψ_3 event planes. The v_3 results are shown in Fig. 2 with v_2 and different theory calculations. Four such predictions shown in Fig. 2 employ viscous hydrodynamics with η/s at or near the conjectured lower bound $1/4\pi$ [15] and one is from the AMPT (A-Multi-Phase-Transport-Model) framework [16]. The SONIC calculation [11] employs Glauber initial conditions, viscous hydrodynamics, and then at $T = 170$ MeV a transition to a hadronic cascade. The SUPERSONIC calculation [13] additionally includes pre-equilibrium dynamics that boosts the initial velocity fields at the earliest times. The impact of pre-equilibrium is modest on the v_2 values and the data agree with both calculations within uncertainties. The effect of pre-equilibrium on v_3 is significantly larger as the triangular flow takes longer to develop [11]. The SUPERSONIC prediction agrees well with the experimental data for $p_T < 1.2$ GeV/c, and then the data trends towards the SONIC prediction at higher p_T.

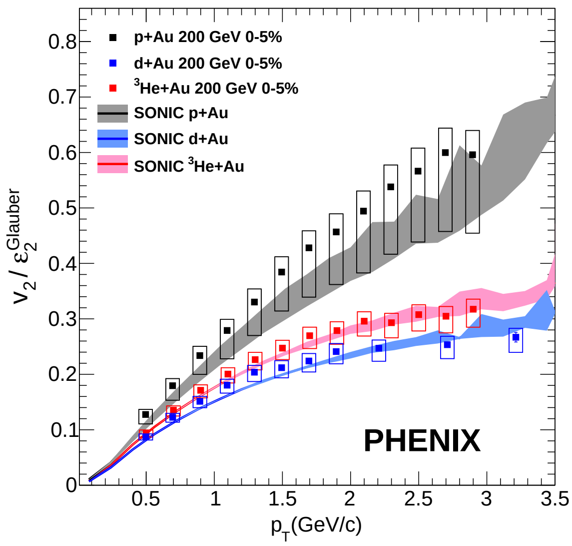

Figure 1: Measured v_2 for mid-rapidity charged tracks in 0-5% central p+Au,d+Au and ^{3}He+Au at $\sqrt{s_{NN}} = 200$ GeV using the event plane method. Also shown are SONIC model calculations [13]

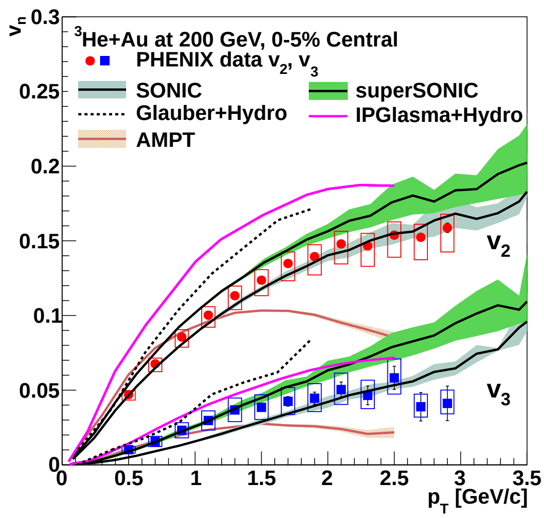

Figure 2: v_2 (circles) and v_3 (squares) as a function of p_T for inclusive charged hadrons at mid-rapidity in 0-5% central ^{3}He+Au collisions at $\sqrt{s_{NN}} = 200$ GeV; Also shown are various theoretical calculations.

3. The v_2 measurements in p+p collisions at $\sqrt{s_{NN}} = 2.76$, 5, 7, and 13 TeV at the LHC

The v_2 in p+p collisions at $\sqrt{s_{NN}} = 2.76$ and 13 TeV has been measured with long-range($|\Delta\eta| > 2$) two particle $\Delta\phi$ correlations by ATLAS [20]. A new method, called template fitting has been developed to separate the ridge and the back-to-back jet correlation in this long-rang two particles correlation, by assuming that the shape of the jet-induced correlations is invariant with event multiplicity and can be extracted from low-multiplicity events. The second order harmonic coefficients $v_{2,2}$ from template fitting and the v_2 extracted by assuming factorization are shown in the Fig 3. Both $v_{2,2}$ and v_2 show a very week multiplicity dependence and are nearly identical for collision energy from 2.76 to 7 TeV.

The anisotropy of charged particles are also measured in p+p collisions at 13 TeV by CMS [17]. A different subtraction method [4] is employed by CMS. The second-order Fourier coefficients

$V_{2\Delta}$ extracted from long-range two-particle $\Delta\phi$ correlations in the higher-multiplicity region are subtracted from the $V_{2\Delta}$ coefficients from $10 \leq N_{\rm trk}^{\rm offline} < 20$ with

$$V_{2\Delta}^{\rm sub} = V_{2\Delta} - V_{2\Delta}(10 \leq N_{\rm trk}^{\rm offline} < 20)\,\frac{N_{\rm assoc}(10 \leq N_{\rm trk}^{\rm offline} < 20)}{N_{\rm assoc}}\,\frac{Y_{\rm jet}}{Y_{\rm jet}(10 \leq N_{\rm trk}^{\rm offline} < 20)}. \quad (1)$$

Here, $Y_{\rm jet}$ represents the near-side jet yield obtained by integrating the difference of the short- and long-range event-normalized associated yields for each multiplicity class as shown for $105 \leq N_{\rm trk}^{\rm offline} < 150$ over $|\Delta\phi| < 1.2$. The ratio, $Y_{\rm jet}/Y_{\rm jet}(10 \leq N_{\rm trk}^{\rm offline} < 20)$, is introduced to account for the enhanced jet correlations resulting from the selection of higher-multiplicity events.

The $V_{2\Delta}$ is shown in the Fig 4 as a function of $N_{\rm trk}^{\rm offline}$ for charged particles. Before subtraction, the $V_{2\Delta}$ coefficients are found to be nearly constant as a function of multiplicity. After subtraction, $V_{2\Delta}$ exhibits an increase with multiplicity for $N_{\rm trk}^{\rm offline} \lesssim 100$. This jet subtraction procedure is also tested in PYTHIA simulations, where no jet modification from initial or final state effects is present. The $V_{2\Delta}$ after subtraction is found to be consistent with zero as shown in the Fig 4.

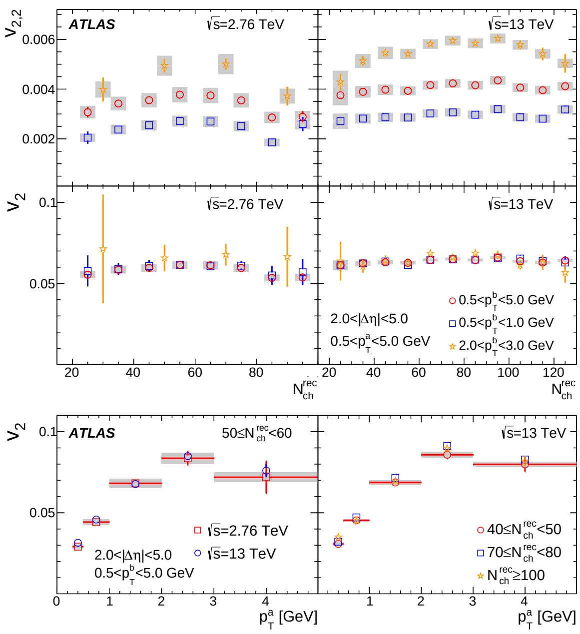

Figure 3: The integral $v_{2,2}$ and v_2 from template fitting as a function of multiplicity in in p+p collisions at $\sqrt{s_{NN}} = 2.76$ TeV(top left) and 7 TeV(top right). The v_2 as a function of p_T are also shown in these two collision energy(bottom left) and different multiplicity bins at 7 TeV.(bottom right)

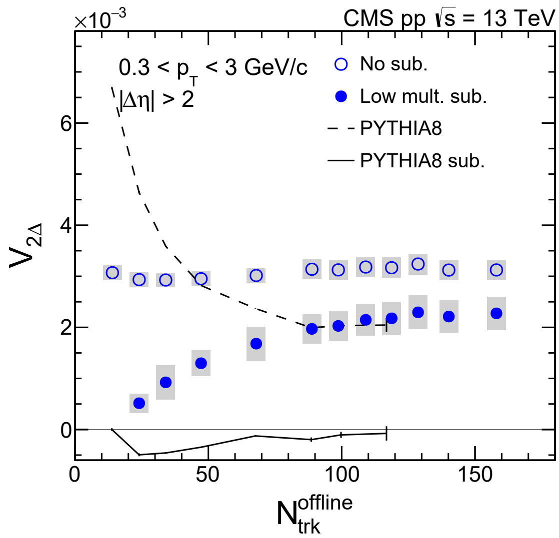

Figure 4: $V_{2\Delta}$ as a function of $N_{\rm trk}^{\rm offline}$ for charged particles, averaged over $0.3 < p_T < 3.0 GeV/c$, in p+p collisions at $\sqrt{s_{NN}} = 13$ TeV, before (open) and after (filled) subtraction of jet correlations, estimated from the $10 \leq N_{\rm trk}^{\rm offline} < 20$ range. Results from PYTHIA are shown as curves.

4. Fourier harmonics from multi-particle correlations

Different methods of jet subtraction will lead to quite different multiplicity dependence for v_2 measurements, as shown by results above. To avoid this uncertainty, CMS also measures the v_2 in p+p collisions by using a multi-particle cumulant method [21]. This technique has the advantage of suppressing short-range two-particle correlations such as jets and resonance decays. The corresponding cumulants, $c_n\{4\}$ and $c_n\{6\}$, are calculated as follows [21]:

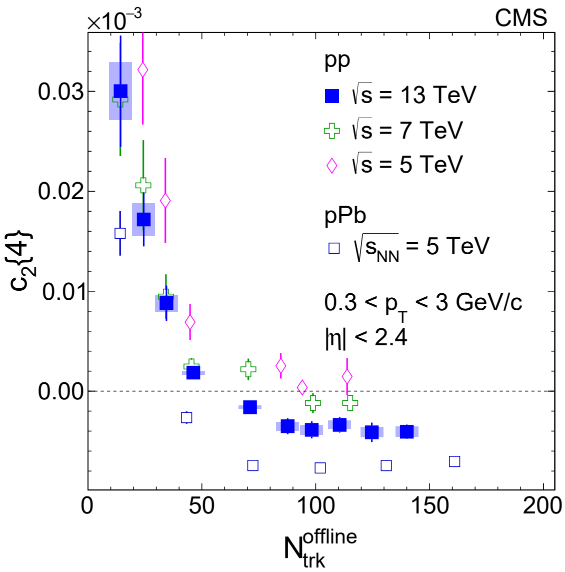

Figure 5: $c_n\{4\}$ as a function of $N_{\rm trk}^{\rm offline}$ for charged particles, averaged over $0.3 < p_T < 3.0 GeV/c$, in p+p collisions at $\sqrt{s_{NN}} = 5$, 7, and 13 TeV. The $c_n\{4\}$ from p+Pb collisions at 5 TeV are also shown for comparison

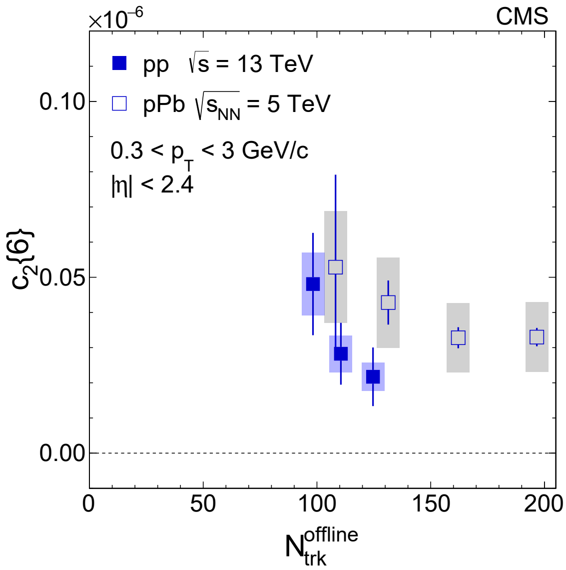

Figure 6: $c_n\{6\}$ as a function of $N_{\rm trk}^{\rm offline}$ for charged particles, averaged over $0.3 < p_T < 3.0 GeV/c$, in p+p collisions at $\sqrt{s_{NN}} = 13$ TeV and compare with that measured in p+Pb collisions at 5 TeV.

$$\begin{aligned} c_n\{4\} =& \langle\langle 4\rangle\rangle - 2\times\langle\langle 2\rangle\rangle^2, \\ c_n\{6\} =& \langle\langle 6\rangle\rangle - 9\times\langle\langle 4\rangle\rangle\langle\langle 2\rangle\rangle + 12\times\langle\langle 2\rangle\rangle^3. \end{aligned} \tag{2}$$

Fig. 5 shows the four-particle cumulant $c_2\{4\}$ values for charged particles($0.3 < p_T < 3.0GeV/c$) as a function of $N_{\rm trk}^{\rm offline}$ for p+p collisions at $\sqrt{s_{NN}} = 5$, 7, and 13 TeV. The p+Pb data at $\sqrt{s_{NN}} = 5$ TeV [4] are also plotted for comparison. The six-particle cumulant $c_2\{6\}$ values for p+p collisions at $\sqrt{s_{NN}} = 13$ TeV are shown in Fig. 6, comparing with p+Pb data at $\sqrt{s_{NN}} = 5$ TeV [4].

Similar to that found for p+Pb collisions, the $c_2\{4\}$ values decrease as a function of increasing multiplicity in p+p collisions for all three collision energies. In p+p collisions at 13 TeV, the $c_2\{4\}$ switches sign from positive to negative at $N_{\rm trk}^{\rm offline}$ above 60, and indicates a collective $v_2\{4\}$ signal [22]. An indication of energy dependence of $c_2\{4\}$ values is seen in Fig. 5, where $c_2\{4\}$ tends to be more positive for a given $N_{\rm trk}^{\rm offline}$ range at lower collision energies. It may be due to different average p_T values at different collisions energies or different multiplicity fluctuations. The positive $c_2\{6\}$ values are also observed in the p+p collisions at 13 TeV which is similar to what was observed in p+Pb collisions

5. The v_2 of identified particles in p+p and ^{3}He+Au collisions

The v_2 of K_S^0 and $\Lambda/\overline{\Lambda}$ particles are measured in the high multiplicity p+p collisions at 13 TeV by CMS [17]. After correction for jet correlations estimated from low-multiplicity data, the $v_2^{\rm sub}$ results as a function of p_T for $105 \le N_{\rm trk}^{\rm offline} < 150$ are shown in Fig. 7 (top). The particle mass ordering of v_2 values is observed in the lower p_T region, while at higher p_T the ordering is reversed. The number of quark scaling as a function of KE_T/n_q is shown in Fig. 7 (bottom) with a dashed curve corresponding to a polynomial fitting to the K^0_S data. The ratio of v_2^{sub}/n_q results for K^0_S and $\Lambda/\overline{\Lambda}$ particles divided by this polynomial function fitting is also shown in Fig. 7 (bottom). An approximate scaling is seen for $KE_T/n_q \gtrsim 0.2GeV$ within about ±10%.

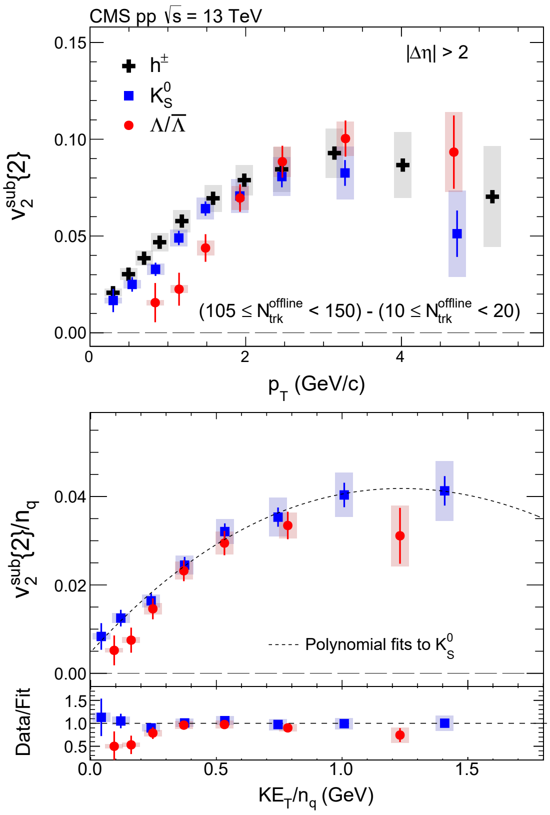

Figure 7: Top: the v_2^{sub} results of inclusive charged particles, K^0_S and $\Lambda/\overline{\Lambda}$ particles as a function of p_T in 13 TeV p+p for multiplicity as $105 \leq N_{trk}^{offline} < 150$, after subtracting jet correlations estimated from low-multiplicity data. Bottom: the v_2^{sub}/n_q for K^0_S and $\Lambda/\overline{\Lambda}$ as a function of KE_T/n_q. Ratios to a smooth fit function of data for K^0_S particles are also shown.

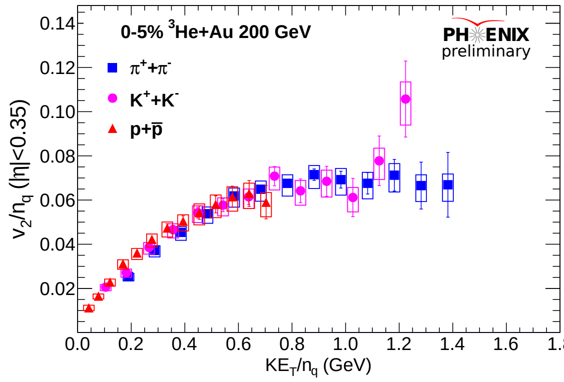

Figure 8: The scaling of number of quark of $v_2(p_T)$ for $\pi^{\pm}$, $K^{\pm}$ and (anti)protons in 0-5% central ^{3}He+Au collisions.

PHENIX measured the v_2 of $\pi^{\pm}$, $K^{\pm}$ and (anti)protons in the central ^{3}He+Au collisions at 200 GeV. Fig. 8 shows the number of quark scaling for v_2 of $\pi^{\pm}$, $K^{\pm}$ and (anti)protons as a function of KE_T/n_q (GeV). The number of quark scaling is found to hold in the small collisions system, which is consistent with viscous hydro calculations or quark coalescence models [18, 19].

6. Summary

I summarize the recent measurements of anisotropy(v_2, v_3) in small collision systems which include p+p, p+A, d+Au and ^{3}He+Au collisions. The v_2 and v_3 are measured with several different ways which include the long-range two particles $\Delta\phi$ correlations, event plane with large η gap and multi-particles cumulant methods. A sizable v_2 and v_3 are observed in the small collision systems and found to be related to the initial geometry. A particle mass ordering of v_2 values are also observed for the identified particles in small collisions. All these measurements are similar to what were observed in large A+A collisions system and indicate a mini-QGP has been generated in small collision systems.

References

[1] Chatrchyan, S *et al.* (CMS Collaboration) 2013 *Phys. Lett. B* **718** 795-814
[2] Aad, G *et al.* (ATLAS Collaboration) 2013 *Phys. Rev. Lett.* **110** 182302
[3] Aad, G *et al.* (ATLAS Collaboration) 2013 *Phys. Lett. B* **725** 60-78
[4] Chatrchyan, S *et al.* (CMS Collaboration) 2013 *Phys. Lett. B* **724** 213-240
[5] Abelev B *et al.* (ALICE Collaboration) 2013 *Phys. Lett. B* **719** 29-41
[6] Adare, A *et al.* (PHENIX Collaboration) 2013 *Phys. Rev. Lett.* **114** 212301
[7] Adare, A *et al.* (PHENIX Collaboration) 2015 *Phys. Rev. Lett.* **114** 192301
[8] Adare, A *et al.* (PHENIX Collaboration) 2015 *Phys. Rev. Lett.* **114** 142301
[9] Dusling, K *et al.* 2013 *Phys. Rev. D* **87** 094034
[10] Bozek, P *et al.* 2012 *Phys. Rev. C* **114** 014911
[11] Nagle, J. *et al.* 2014 *Phys. Rev. Lett.* **114** 112301
[12] Heikki Möntysaari, Björn Schenke, arxiv: 1603.04349
[13] Paul Romatschke, arxiv: 1502.04745
[14] Aidala, C *et al.* arXiv: 1311.3594
[15] Kovtun, P *et al.* 2005 *Phys. Rev. Lett.* **94** 111601
[16] Lin, Z.-W. Lin *et al.* 2005 *Phys. Rev. C* **72** 064901
[17] Chatrchyan, S *et al.* (CMS Collaboration) arXiv: 1606.06198
[18] Hwa, Rudolph C., Yang, C. B., 2003 *Phys. Rev. C* **67** 034902
[19] Fries, R. J. *et al.* 2003 *Phys. Rev. Lett.* **90** 202303
[20] Aad, G *et al.* (ATLAS Collaboration) 2016 *Phys. Rev. Lett.* **116** 172301
[21] Bilandzic, A *et al.* 2011 *Phys. Rev. C* **83** 044913
[22] Borghini, N *et al.* 2011 *Phys. Rev. C* **63** 054906